ELSEVIER

Catalysis Today 62 (2000) 355–366

CATALYSIS TODAY

www.elsevier.com/locate/cattod

Catalytic hydrodehalogenation as a detoxification methodology

Claudia Menini, Colin Park, Eun-Jae Shin[1], George Tavoularis, Mark A. Keane*

Department of Chemical Engineering, The University of Leeds, Leeds LS2 9JT, UK

Abstract

Catalytic hydrodehalogenation is presented as a viable approach in the non-destructive treatment of concentrated halogenated aromatic gas streams to generate reusable raw material. Nickel loaded (from 1.5 to 20.3% w/w) silica catalysts have been used to hydrotreat a range of halogenated feedstock, where $473\,K \leq T \leq 573\,K$: chlorobenzene, chlorotoluene, chlorophenol, bromobenzene, dichlorobenzene, dichlorophenol, trichlorophenol, pentachlorophenol. The long term (up to 800 h-on-stream) stability of these catalysts has been assessed where the changes in nickel particle size and morphology as a result of the prolonged catalytic step was probed by TEM; each catalyst irrespective of any loss of initial activity was fully selective in solely promoting dehalogenation. In the case of a polychlorinated feedstock, dechlorination can proceed in a stepwise manner to generate a partially dechlorinated product. Hydrodehalogenation appears to occur via an electrophilic mechanism where the presence of electron-donating substituents on the benzene ring enhances the rate of reaction. The reaction is shown to be structure sensitive over Ni/SiO_2 where the hydrodechlorination rates and ultimate yield of the parent aromatic from a polychlorinated reactant is favored by larger nickel particle sizes. A direct contact of the freshly activated catalyst with HCl or HBr gas induced an appreciable growth of the supported metal crystallites. Chlorobenzene hydrodechlorination was suppressed on a HCl or HBr treated Ni/SiO_2 which promoted instead the unexpected growth of highly ordered carbon filaments; this carbon growth is characterized by TEM and SEM. The dependence of the experimental hydrodechlorination and hydrodebromination rates on the gas phase aromatic partial pressure (in the range 0.02–0.1 atm) is adequately represented by a kinetic model involving a non-competitive adsorption of hydrogen and halogenated aromatic where the incoming aromatic reactant must displace the hydrogen halide from the catalyst surface.

Keywords: Catalytic hydrodechlorination; Catalytic hydrodebromination; Nickel/silica; Structure sensitivity; Dehalogenation kinetics; Catalyst deactivation; Graphitic carbon growth

1. Introduction

Halogenated aromatic compounds exhibit high toxicity and have long been regarded as a major source of environmental pollution [1,2]. To date, incineration has largely been the preferred methodology for handling, or rather disposing of, such organic waste but the requisite high destruction/removal efficiency (>99.9999%) is difficult to achieve when dealing with halogenated aromatics [3]. Moreover, incineration can generate highly toxic polyhalogenated dibenzofurans and dibenzodioxins [4,5] largely as a result of a reduction in the temperature of the residual gases in the vent. Incineration costs are based on halogen content and are ever increasing which, allied to prohibitive legislation [6], will soon render incineration as an unfeasible option. Non-thermal technologies which include [7–9] direct adsorption on activated carbon, solvent extraction, use of ionizing radiation and microbial degradation do not constitute exhaustive

* Corresponding address. Department of Chemical and Materials Engineering, University of Kentucky, Lexington KY 40506-0046, USA.

[1] National Renewable Energy Laboratory, Golden, CO 80401-3393, USA

0920-5861/00/$ – see front matter
PII: S0920-5861(00)00437-5

solutions. Solvent extraction/carbon adsorption only offer means of concentration and if the extracted component is a mixture of chlorinated isomers, these are not, without some difficulty, recovered for reuse. Biological treatment is capable of degrading organochlorine compounds but the rates of conversion are low necessitating the construction of oversized and expensive reactors. Catalytic hydrodechlorination represents an alternative and innovative approach whereby the hazardous material is transformed into recyclable products in a closed system with limited toxic emissions. From an economic viewpoint, taking incineration as the principal means of treatment, a move to a catalytic hydrogen treatment represents immediate savings in terms of fuel and/or chemical recovery. Indeed, Kalnes and James [10] in a pilot-scale study clearly showed the appreciable economic advantages of hydrodechlorination over incineration. Moreover, mixed isomers arising from "uncontrolled" chlorination reactions can be converted back to the single parent raw material precursor from which they originated or to some target partially dechlorinated isomer, in short a unique process of chemical synthesis.

While catalytic hydroprocessing is well established, catalytic hydrodehalogenation is still in a formative stage. Nevertheless, the catalytic hydrodechlorination of chlorobenzene and chlorophenol(s), as model reactants, has been reported both in the gas [11–25] and liquid [26–30] phases using palladium [18–20,27–30], platinum [26,27], rhodium [19,20,27] and nickel [11,12–17,21–25] based catalysts. The treatment of bromobenzenes has not been studied to the same extent and few published accounts could be found. The significant reports have focused on liquid phase reactions with Wei et al. [31] employing metallocenyl diphosphine complexes in a homogeneous catalysis application, Yu et al. [32] using a polymer-anchored Pd catalyst for hydrodebrominations in ethanol while Armedia et al. [33] found that Pd supported on $SiO_2/AlPO_4$, ZrO_2 and MgO was active in liquid phase transformations. Gas phase debromination has been touched upon as addenda to the main thrust of the studies undertaken by Kraus and Bazant [18] and Moreau et al. [34]. Hydroprocessing of polychlorinated aromatics, particularly multiple chlorine removal from a parent phenol has received scant attention in the literature. Limited reaction data are, nonetheless, available for the hydrodechlorination of dichlorophenols in the gas [23,24,35] and liquid [30] phase. The database for catalytic hydrodechlorination is certainly expanding if one compares the contents of review articles dating from 1980 [36] and 1996 [37]. The majority of the published studies have involved a compilation of rate data to characterize individual metal/halo-reactant systems and the mechanism of carbon–halogen bond hydrogenolysis from an aromatic host is still open to question. Catalyst deactivation during hydrodehalogenation has been noted in several instances [14,17,22,26,32,33,38] and attributed to either coke formation [14,26] or poisoning by the hydrogen halide that is formed [14,22,32,38]. However, the effects of halogen/metal interactions on catalyst structure have still to be investigated in a comprehensive fashion. There is also a need for fundamental kinetic studies and there have been few attempts [12,14,18,19] to construct kinetic models that are based on mechanistic considerations. In this paper, we set out to assess the viability of employing supported nickel catalysts (Ni/SiO_2) to hydrodehalogenate mono-chlorobenzene, mono-chlorotoluene, mono-chlorophenol, mono-bromobenzene and polychlorinated phenols. Catalyst durability is considered, the possibility of structure sensitivity is probed, changes to metal dispersion during catalysis are examined and kinetic/mechanistic features are discussed. The nature of catalyst deactivation is examined and preliminary characterization results for an unexpected growth of highly ordered carbon during hydrodechlorination are also provided.

2. Experimental

2.1. Catalyst preparation, activation and characterization

Five silica-supported (Cab-O-Sil 5M, BET surface area $= 194\,m^2\,g^{-1}$) nickel catalysts of varying nickel loading (in the range 1.5–20.3% w/w) were prepared by homogeneous precipitation/deposition as described in detail elsewhere [39]. The hydrated samples, sieved in the 150–200 μm mesh range, were reduced, without a precalcination step, by heating in a $100\,cm^3\,min^{-1}$ stream of dry hydrogen (99.9%) at a fixed rate of $5\,K\,min^{-1}$ (controlled using a Eurotherm 91 e temperature programmer) to a final temperature

of 673 ± 1 K which was maintained for 18 h. The activation (and reaction) temperature was monitored and controlled by a thermocouple inserted in a thermowell within the catalyst bed, reactor temperature was constant to within ±1 K. The nickel content (accurate to within ±2%) was measured by atomic absorption spectrophotometry (Perkin Elmer 360 spectrophotometer) and the water contents were determined by thermogravimetry (Pye Unicam thermobalance) [40], water content was less than 5% w/w. Selected catalyst samples were contacted with flowing HCl and HBr gas (in the range 20–150 $cm^3\,min^{-1}$ for 0.25–5 min) at 548 K. The HCl/HBr contact was exothermic and gave rise to an increase in catalyst bed temperature by up to 34 K. The freshly activated and pretreated catalyst samples were analyzed by transmission electron microscopy (TEM) using a Philips CM20 TEM operated at an accelerating voltage of 200 KeV. The specimens were prepared by suspending the catalyst in isopropyl alcohol with ultrasound, evaporating a drop of the resultant suspension onto a 'holey' carbon support grid. The particle size distribution profiles presented in this study are based on a measurement of over 500 individual particles. The average particle sizes obtained from TEM analysis did not diverge by more than ±15% from the values obtained from CO chemisorption [39]. Scanning electron microscopic (SEM) analysis was performed on a Hitachi S700 field emission SEM where the sample was deposited on a standard SEM holder and double coated with gold.

2.2. Catalytic reactor system

All the catalytic reactions were carried out under atmospheric pressure, in situ immediately after the activation step, in a fixed bed glass reactor (ratio of catalyst particle to reactor diameter = 0.12) over the temperature range 473 K ≤ T ≤ 573 K. The catalyst was supported on a glass frit and a layer of glass beads above the catalyst bed served as a preheating zone and ensured that the reactants reached the reaction temperature before contacting the catalyst. The catalytic reactor has been described previously in some detail [41,42] but the pertinent features are given below. A Model 100 (kd Scientific) microprocessor controlled infusion pump and a Merck–Hitachi LC-6000A pump were used to deliver the halogenated feed via a glass/teflon air-tight syringe and teflon line over a range of volumetric feed rates and the vapor was carried through the catalyst bed in a stream of purified hydrogen, the flow rate of which was monitored using a Humonics (Model 520) digital flowmeter. Undiluted chlorobenzene (CB, Aldrich, >99.9%) chlorotoluene (CT, Aldrich, 99%) and bromobenzene (BB, Aldrich, >99.9%) and methanolic solutions of selected chlorophenol (CP, Aldrich, >99.9%), dichlorobenzene (DCB, Aldrich, >99.9%) dichlorophenol (DCP, Aldrich, >99.9%) and trichlorophenol (TCP, Aldrich, 99%) isomers and pentachlorophenol (PCP, Aldrich, 98%) served as feedstock. Passage of each reactant feed in a stream of hydrogen through the empty reactor did not result in any detectable conversion. The catalytic measurements were made at an overall gas space velocity of 2250 h^{-1} where the partial pressure of hydrogen was maintained at 0.9 atm while the CB and BB partial pressure were varied in the range 0.02–0.1 atm. The catalytic system has been shown [15] to operate with negligible diffusion retardation of the reaction rate under the stated conditions; effectiveness factor (η) >0.9999 at 573 K. Heat transport effects can also be disregarded when applying the criteria set down by Mears [43].

The reactor effluent was frozen in a liquid nitrogen trap for subsequent analysis which was made using an AI Cambridge GC94 chromatograph equipped with a split/splitless injector and a flame ionization detector, employing a DB-1 50 m × 0.20 mm i.d., 0.33 μm capillary column (J&W Scientific), data acquisition and analysis were performed using the JCL 6000 (for Windows) chromatography data system converting peak area to mole fraction using detailed (20 point) calibration plots. Quantitative analysis was based on relative peak area with acetone as solvent where reproducibility was better than ±0.1% and the detection limit typically corresponded to a feedstock conversion less than 0.1 mol%. A chlorine (in the form of HCl product) mass balance was performed by passing the effluent gas through an aqueous NaOH ($3.5–8.0 \times 10^{-3}$ mol dm^{-3}, kept under constant agitation at ≥300 rpm) trap and monitoring continuously the pH change by means of a Hanna HI Programmable Printing pH Bench-Meter. The concentration of HCl generated was also monitored by titrimetric analysis of the NaOH trap solution; chlorine mass balance was complete to better than ±10%. Qualitative analysis for the presence of chlorine gas was made by

analysis of the trap for the formation of hydrates at $T > 283\,K$ [44]. The test was negative in every instance which confirms that hydrogenolytic cleavage of halogen substituents from an aromatic host yields the corresponding hydrogen halide as the only inorganic product. At the end of each catalytic run the catalyst was normally heated in flowing dry hydrogen at $5\,K\,min^{-1}$ to 673 K and maintained at this temperature for at least 12 h. In many instances the reaction was repeated under identical conditions where rate reproducibility was better than ±7%.

3. Results and discussion

The gas phase hydrodechlorination of chlorobenzene (CB) over the range of reactant partial pressures, temperatures and nickel metal loadings that were considered generated benzene and HCl as the only detected products. The conversion of bromobenzene (BB) likewise yielded only benzene and HBr and aromatic ring reduction, in both instances, can be positively discounted. The catalytic hydrogen treatment of each chlorophenol (CP) isomer generated only phenol and HCl and there was no detectable formation of cyclohexanone or cyclohexanol as a result of a further hydrogenation of phenol. A minor degree of CP isomerization activity (<1 mol% conversion) was evident in this study but we did not isolate even trace amounts of benzene or chlorobenzene in contrast to the results reported by Chon and Allen for a Ni/Mo–Al_2O_3 catalyst [12]. A selective hydrodechlorination is to be expected given the reported [45] bond dissociation energies of aromatic C–Cl ($406\,kJ\,mol^{-1}$) and C–OH ($469\,kJ\,mol^{-1}$) which show that the hydrodeoxygenation step is the more energetically demanding.

Catalyst durability in the continuous single pass hydrodechlorination of chlorobenzene over two Ni/SiO_2 catalysts bearing a low and high nickel loading is assessed in Fig. 1 wherein the ratio of the fractional conversion at a particular time-on-stream (x_{Cl}) to the initial conversion over a freshly activated catalyst (x_0) is related to process time. The data plotted in Fig. 1 were obtained from periodic sampling of the effluent stream for up to 800 h of continual operation which represents, for the lower nickel loaded sample, a total chlorine to nickel mole ratio of 2×10^4:1. The nickel-dilute catalyst, albeit there is a decided scatter

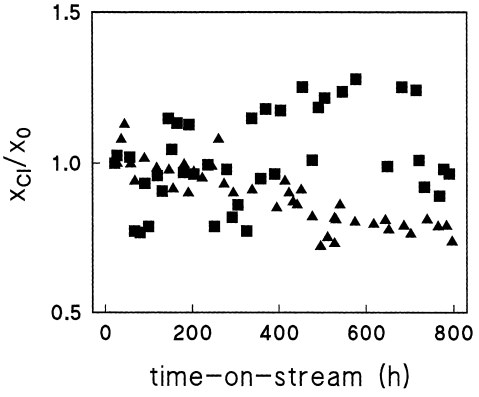

Fig. 1. Variation of the ratio of time dependent (x_{Cl}) to initial (x_0) fractional conversion of CB at 573 K as a function of time-on-stream over 1.5% w/w (■) and 15.2% w/w (▲) Ni/SiO_2.

of experimental data, largely retained its initial activity while the higher loaded catalyst exhibited a discernible decline in conversion with prolonged use. The latter catalyst still delivered an appreciable degree of conversion and remained fully selective in terms of solely promoting benzene formation but the initial activity ultimately fell by a factor of 0.7. The possible involvement of a nickel particle size effect is probed in Fig. 2 where the specific hydrodechlorination rate (per exposed nickel surface area) in the conversion of CB and 2-CP is plotted as a function of nickel particle size. An increase in the supported nickel particle size consistently generated, for both feedstock, a higher specific chlorine removal rate. The nickel particle sizes consi-

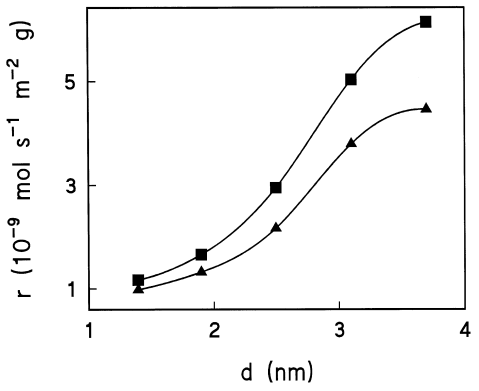

Fig. 2. Specific hydrodechlorination rate as a function of nickel particle size for the conversion of CB (▲) and 2-CP (■) at 573 K.

Table 1
Phenol yield (Y) from the hydroprocessing of a range of polychlorinated phenolic feedstock over three nickel loaded silica catalysts at 573 K[a]

Reactant	% Ni w/w	Y (%)
2,6-DCP	1.5	5
2,6-DCP	11.9	21
2,6-DCP	20.3	29
2,4,5-TCP	1.5	5
2,4,5-TCP	11.9	16
2,4,5-TCP	20.3	24
PCP	1.5	4
PCP	11.9	13
PCP	20.3	19

[a] $x = 0.30 \pm 0.06$.The concentration of surface nickel sites was kept constant in the three catalyst beds.

dered in this study fall within the so-called mitohedrical [46] region wherein catalytic reactivity can show a critical dependence on morphology. However, Estelle et al. [17] also noted evidence of structure sensitivity in hydrodechlorination over unsupported nickel catalysts. The observed antipathetic structure sensitivity with larger supported particles having a higher activity than smaller ones supports the existence of some form of ensemble effect. Coq et al. [19], on the other hand, have reported that CB dechlorination is enhanced over smaller palladium and rhodium particles. The yield of phenol from a polychlorinated feedstock was also found, in this study, to be particle size dependent as shown in Table 1 where complete removal of the chlorine complement to produce phenol was favored in every case at higher nickel loadings.

Hydodehalogenation has been viewed in terms of both a nucleophilic [18,47] and electrophilic [11,12,22,23] attack of hydrogen on the adsorbed halo-aromatic. There is general agreement in the literature that the reactive hydrogen is adsorbed dissociatively [14,15,17–20,48] while the involvement of spillover species has also been proposed [14,48]. The effect of aromatic ring substitution, with varying associated electron-donor/acceptor properties, on the rate of single hydrodechlorination steps under identical reaction conditions is illustrated in Table 2. The observed increase in dechlorination rate in moving from a strongly electron-withdrawing substituent (–Cl in 1,4-DCB and 2,3-DCP) to the elctron donating –OH (in 3-CP) and $–CH_3$ (in 3-CT) is diagnostic of

Table 2
Hydrodehalogenation rates at 548 K over 1.5% w/w Ni/SiO_2 for selected single halogen removal steps[a]

Dehalogenation step	r (10^{-3} mol h^{-1} g^{-1})
CB → benzene	2.9
3-CP → phenol	5.0
3-CT → toluene	4.3
1,4-DCB → CB	1.5
2,3-DCP → CP	1.9
BB → benzene	0.9

[a] Inlet partial pressure of halogenated reactant = 0.04 atm.

an electrophilic mechanism. This would presume that the aromatic ring in the transition state is cationic with respect to the initial state and electropositive substituents lower the activation barrier by stabilizing the transition state. The lower rate of hydrodebromination (of BB) relative to that of hydrodechlorination (of CB) suggests a less effective activation of the C–Br bond for attack by hydrogen. This may be explained on the basis of the lower electron affinity of bromine compared with chlorine [49] that translates into a reduced strength of adsorption and poorer activation. In terms of the prevalent surface steps, as a first approach we assume that adsorption of both reactants is non-competitive. The latter does find support in the fact that the reaction order with respect to CB has been shown elsewhere [15] to be independent of the partial pressure of hydrogen. Taking hydrogen adsorption to be dissociative on sites Z'

$$H_2(g) + Z' \rightleftharpoons 2H\text{-}Z'$$

where adsorption is in equilibrium (K_1) and the surface hydrogen reacts with chlorobenzene (as a representative case) adsorbed on separate (Z) sites in an irreversible step (k)

$$CB\text{-}Z + 2H\text{-}Z' \rightarrow B(g) + HCl\text{-}Z + 2Z'$$

Under these reaction conditions each dehalogenation step is thermodynamically very favorable [15,23] and the recorded conversions are far removed from equilibrium. The chloroaromatic adsorption involves a direct "catalytically significant" interaction of the chlorine component with the surface and the HCl that remains on the catalyst is displaced by incoming CB in an equilibrated step (K_2)

$$CB(g) + HCl\text{-}Z \rightleftharpoons CB\text{-}Z + HCl(g)$$

The rate expression that follows from the above steps is given by

$$r = \frac{kK_1 P_{CB} P_{H_2}/P_{HCl}}{K_2^{-1} + P_{CB}/P_{HCl}}$$

The predicted (using the above expression) and experimentally determined steady state hydrodechlorination and hydrodebromination rates as a function aromatic partial pressure are compared in Fig. 3, the rates of hydrodebromination at 473 K were too low to be measured accurately. In every instance the dehalogenation rates were elevated with increasing partial pressure (over the range considered in this study) and the catalyst delivered a consistently greater degree of hydrodechlorination. The value of the K_2 parameter was significantly lower for BB (3×10^{-3} at 523 K) when compared with CB (0.16) under the same conditions which is indicative of a weaker interaction with the surface. The percentage deviation predicted from experimental rates is presented in Fig. 4 where the fit to the BB results is inferior; percentage deviation is not greater than ±18%. The model does provide a good

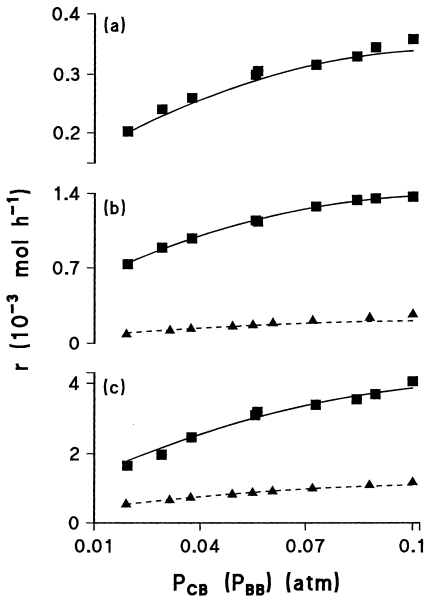

Fig. 3. Variation of the experimentally determined and calculated CB (solid lines) hydrodechlorination (■) and BB (dotted lines) hydrodebromination (▲) rates with varying CB (and BB) partial pressure at (a) 473 K; (b) 523 K; (c) 573 K. $P_{HCl} = 0.001 - 0.03$ atm; $P_{HBr} = 0.0007 - 0.009$ atm.

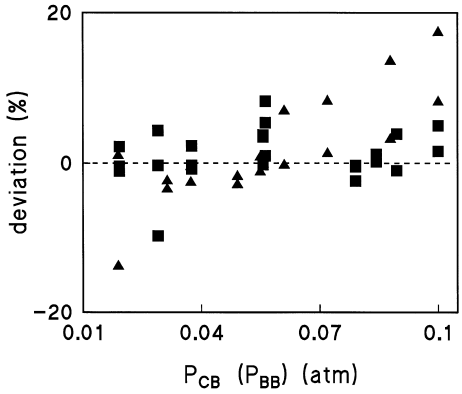

Fig. 4. Deviation (%) of predicted from calculated CB hydrodechlorination (■) and BB hydrodebromination (▲) rates as a function of aromatic partial pressure.

representation of the experimental data over the stated process conditions. While the kinetic expression is reliable it alone can not accredit the associated reaction mechanism. It is recognized that a significant deviation may result over a wider range of aromatic partial pressures or at lower initial hydrogen pressures. Work is ongoing to consider other mechanistic based kinetic models and to extend the input database of experimental rates over a wider range of reaction conditions.

While the supported nickel systems employed in this study did not exhibit any short term decline in hydrodehalogenation activity, there was an evident drop in rate (depicted in Fig. 1) for the higher metal loadings with prolonged and continuous use. Loss of dechlorination activity has been attributed elsewhere [14,22,32,38] to a poisoning or site-blocking effect by the HCl that is produced. It is worth noting that Coq et al. [19] observed a greater resistance to poisoning, during CB hydrodechlorination, with increasing particle size in the case of supported palladium catalysts. The chlorine and bromine coverage of a low (1.5% w/w) and high (15.2% w/w) loaded Ni/SiO_2 was probed by monitoring, via pH changes in the NaOH scrubbing solution, the desorption of HCl and HBr after completion of the catalysis step. The number of moles of HCl and HBr desorbed after a series of catalytic reactions at different aromatic partial pressures and reaction temperatures are recorded in Table 3. In every instance the number of moles of hydrogen halide desorbed from the catalyst exceeded the number of exposed surface nickel sites regardless of

Table 3
Moles of HCl and HBr desorbed from 1.5 and 15.2% w/w Ni/SiO_2 after a series of CB and BB hydrodehalogenation reactions

% Ni w/w	Hydrodehalogenation reaction	$T_{reaction}$ (K)	CB/BB converted (10^2 mol)	Hydrogen halide desorbed (10^5 mol)
1.5	CB → benzene	523	3	12
1.5	CB → benzene	573	14	9
1.5	CB → benzene	573	18	13
1.5	BB → benzene	548	4	11
1.5	BB → benzene	573	6	10
15.2	CB → benzene	523	8	51
15.2	CB → benzene	523	6	46
15.2	CB → benzene	573	29	57
15.2	BB → benzene	523	6	53
15.2	BB → benzene	573	9	48
15.2	BB → benzene	573	14	53

the nickel loading. Surface coverage by HCl and HBr alone cannot account for any loss of initial activity and under reaction conditions the catalyst surface is, in effect, saturated with hydrogen halide. The nickel particle size distribution was however shifted to higher values after extended catalyst use as is illustrated by the histograms presented in Fig. 5. An agglomeration of palladium metal particles (supported on TiO_2, SiO_2, ZrO_2 and Al_2O_3) was also observed by Gampine and Eyman [38] after a series of gas phase hydrodechlorination reactions. The freshly activated (15.2% w/w Ni) catalyst is characterized by a narrow particle size distribution to give a surface weighted average diameter equal to 1.7 nm. The catalysts used in this study have been shown [39] to exhibit strong metal/support interactions which result in a narrow distribution of small particles (<4 nm) after activation. A direct contact of the freshly activated catalyst with

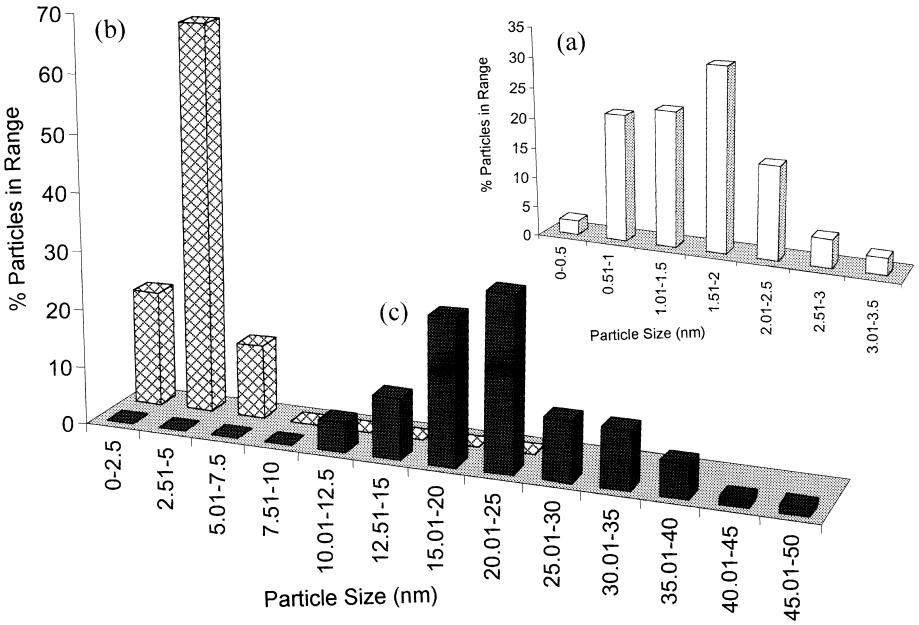

Fig. 5. Nickel particle size distribution in (a) freshly activated catalyst sample (open bars); (b) after extended use in the hydrodechlorination of CB (cross-hatched bars); (c) after contact with HCl gas (solid bars). 15.2% w/w Ni/SiO_2.

HCl gas served to shift the particle size distribution to an appreciably wider range of larger crystallites (see Fig. 5), the surface weighted average is calculated to equal 22.7 nm. Moreover, the HCl treatment resulted in a complete change in nickel particle morphology and an array of geometrically shaped crystallites of varying size was observed by TEM and is illustrated by the micrographs given in Fig. 6. An agglomeration of nickel particles (supported on carbon) after a HCl treatment has been noted elsewhere [50] and was attributed to a surface mobility of Ni–Cl species. Moreover, larger nickel particles are typically generated with a nickel chloride precursor, regardless of the nature of the support or reduction temperature, due to crystallite growth involving volatile nickel chloride in the presence of hydrogen and hydrogen chloride [51]. There was no evidence of any significant metal particle growth in the nickel dilute samples. The HCl treatment also served to lower the dechlorination rate by a factor of 20. This loss of conversion was irreversible in that an attempted reactivation of the catalyst in flowing hydrogen at 673 K over extended periods did not restore the activity to any appreciable degree.

The shift in nickel particle size after HCl treatment was accompanied by the unexpected growth of filamentous carbon during the ensuing catalysis step as shown in Fig. 6. The nature of this carbon growth is perhaps better illustrated by the low and high magnification SEM micrographs given in Fig. 7 that show a multi-point growth of carbon filaments from a catalyst surface that had, in this case, been modified by contact with HBr. These carbon filaments are highly ordered and exhibit little or no curvature, the lattice structure of an isolated carbon filament grown from the HBr treated surface is evident in the TEM shown in Fig. 8. The diameter (and distribution of diameter sizes) of the filaments grown on a range of catalyst surfaces correspond, in every instance, to the dimensions of the surface nickel metal suggesting that the carbon is growing directly from the metal sites. As a consequence of the strong metal/support interaction(s) in these catalysts the metal crystallites remain anchored to the silica and the carbon filaments grow from the

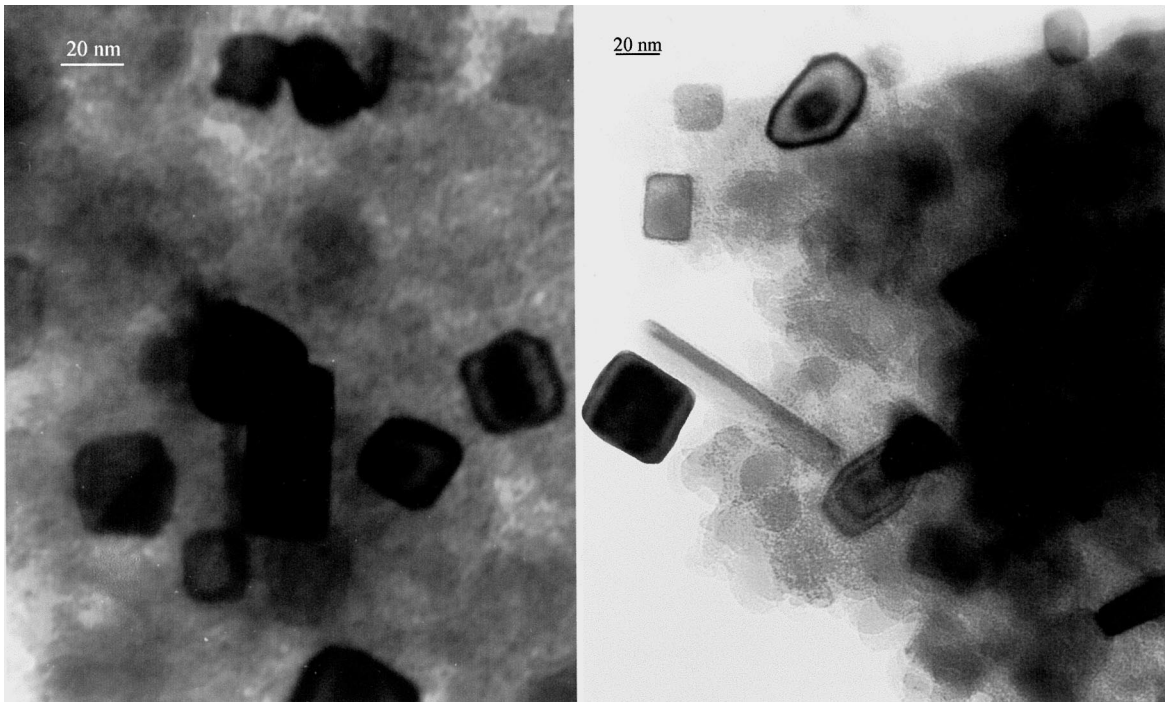

Fig. 6. TEM of the 15.2% w/w Ni/SiO_2 after contact with HCl gas and 12 h-on-stream CB hydrodechlorination at 523 K. Note: filamentous carbon growth is evident in the right hand micrograph.

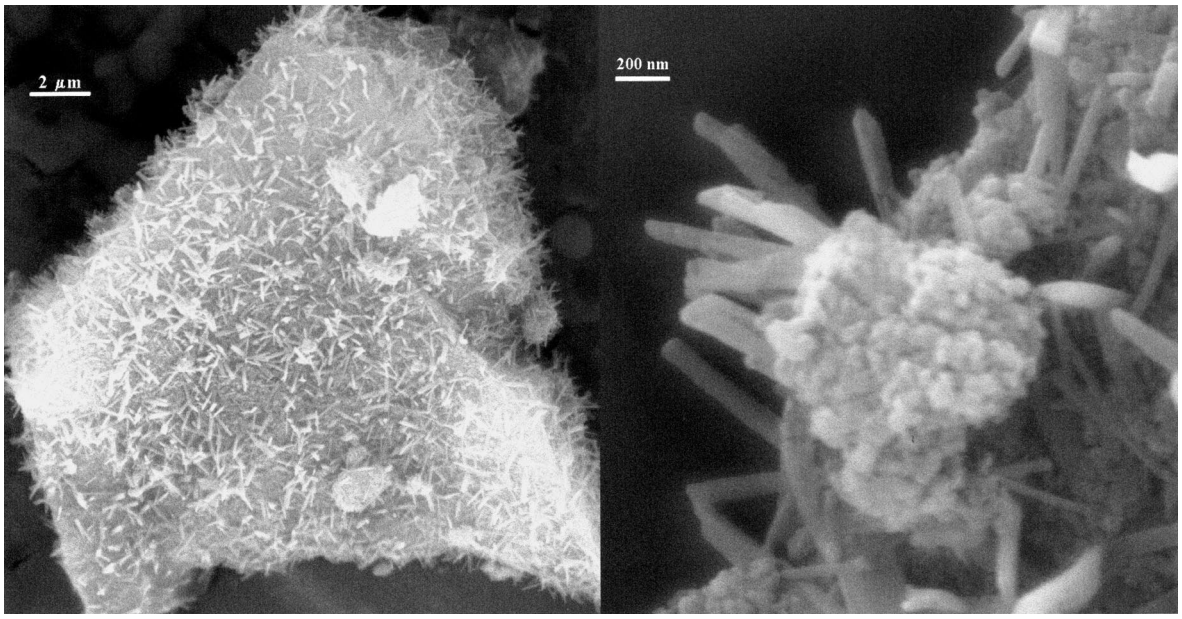

Fig. 7. Low and high magnification SEMs showing the carbon filament growth during the hydrodechlorination of CB at 553 K over a HBr treated 15.2% w/w Ni/SiO_2 catalyst.

exposed faces. The growth of ordered carbonaceous material via catalysis is well established but typically involves an unsaturated hydrocarbon feedstock at temperatures in excess 723 K [52,53]. Carbon growth is initiated by a concomitant adsorption and decomposition of the hydrocarbon on specific faces of the metal followed by a dissolution of the carbon atoms into the metal particle and diffusion at other faces as graphitic layers. The growth and characteristics of the carbon is very much dependent on catalyst composition and the reaction conditions. There was no evidence of such ordered carbon growth on the used catalyst samples that had not been contacted directly with HCl or HBr. The spent (% w/w Ni $>$ 1.5) catalysts did however exhibit an appreciable lay down of amorphous carbon or coke and preliminary XPS analysis has revealed the presence of a surface "nickel carbide" species. Temperature programmed oxidation, in a 5% v/v O_2/He flow, of the used and demineralized catalyst samples revealed an amorphous carbon content of up to 8% w/w. Carbon deposition may in fact be responsible for the gradual loss of activity in the higher nickel loaded catalysts where the effect is cumulative as more of the active phase is occluded by coke deposits. Indeed, the dispersion and morphology of supported metal particles can have a large effect on coke deposition during catalysis [54] and the larger nickel particles may be more prone to coking during hydrodehalogenation. In any case, the generation of ordered carbon filaments from these catalysts was only induced after a direct contact with gaseous hydrogen halide. Chlorine is known to act as an electron acceptor with respect to transition metals [19,55] and the presence of residual chlorine has been shown to disrupt the hydrogen chemisorption characteristics of nickel [14,56], the source of this low temperature carbon growth must be electronic in nature. The direct interaction of the hydrogen halide with the catalyst results in a complete reconstruction of the metal crystallites which may expose orientations that promote the growth of ordered carbon. The presence of the hydrogen halide on the surface must modify the electron density at the metal sites with the result that a dissociative (or destructive) chemisorption of CB is favored. This proposal finds support in the work of Chambers and Baker [57] who reported that trace amounts of chlorine in an ethylene feed promoted the carbon deposition activity (at 673 K) of cobalt and iron powders.

Once the Ni/SiO_2 catalysts had been contacted with HCl and HBr gas, hydrodechlorination activity

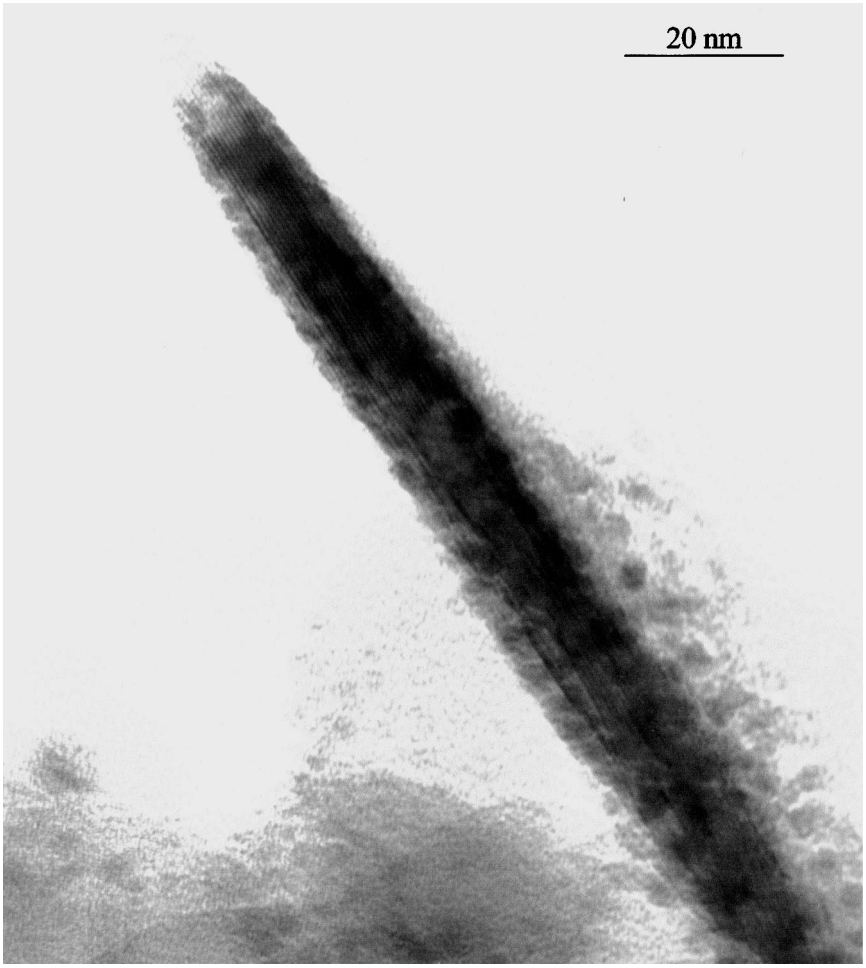

Fig. 8. TEM of an isolated carbon filament grown during the hydrodechlorination of CB at 553 K over a HBr treated 15.2% w/w Ni/SiO_2 catalyst.

was almost completely suppressed and the catalysts promoted predominantly the formation of carbon filaments. It is true that this shift in selectivity is detrimental in terms of our initial intention of developing stable and selective hydrodehalogenation catalysts. Furthermore, the changes that are wrought due to a direct interaction of the hydrogen halide with the catalyst are so extreme that they do not mimic, in a meaningful way, any surface effects during the catalytic step. Nevertheless, this serendipitous low temperature growth of highly ordered carbon can be turned to good effect in terms of adsorption applications. We are now attempting to optimize the growth of this ordered carbon that will then be assessed in terms of adsorption capacity in the uptake of halogenated aromatics. The application of catalysis to the abatement of pollution by haloarenes can now follow two routes, a two-pronged approach: (i) a direct conversion of "halogenated waste" to reusable feedstock or some target isomeric product; (ii) a transformation of the same waste into a potential adsorbent material that can then be used, in turn, to concentrate halogenated waste in a "separations application".

4. Conclusions

Nickel supported on silica promotes the hydrodehalogenation of a range of halogenated aromatics in

temperature range 473–573 K where ring hydrogenation and non-halogen substituent hydrogenolysis steps are not observed. Hydrodehalogenation proceeds via an electrophilic mechanism where the presence of electron donating ring substituents raises the overall reaction rate. The reaction is structure sensitive in that the specific dechlorination rate and complete dechlorination to the parent aromatic are favored by larger nickel metal particles. Under reaction conditions the catalyst surface is saturated with hydrogen halide that is displaced by incoming reactant. While the nickel dilute samples (1.5% w/w) retain the initial activity over prolonged (up to 800 h) periods, the higher loaded catalysts exhibit a gradual decline in activity. The latter can be attributed to halogen/nickel interactions that lead to a growth of the supported metal phase and may influence a more prevalent coking in the case of the larger nickel particles. A direct contact of the freshly activated catalysts with HCl or HBr gas serves to diminish the ensuing hydrodechlorination activity but promote the growth of filamentous carbon from the catalyst surface. Such a pretreatment results in a complete restructuring of the supported metal phase leading to a destructive chemisorption of the halogenated reactant and the formation of highly ordered carbon at an abnormally low temperature.

Acknowledgements

This work has been supported by a grant (GR/M5-1420) from the Engineering and Physical Sciences Research Council (EPSRC). CM also acknowledges partial support from EPSRC (Quota Studentship No. 97302706). The authors wish to thank Dr. R. Brydson for his assistance with the TEM/SEM analyses.

References

[1] C.S. Fang, S.L. Khor, Environ. Prog. 8 (1989) 270.
[2] B.J. Alloway, D.C. Ayres, Chemical Principles of Environmental Pollution, Blackie, Glasgow, 1993.
[3] A. Converti, M. Zilli, D.M. De Favari, G. Ferraiola, J. Hazard. Mater. 27 (1991) 127.
[4] H. R Bauser, Chemosphere 7 (1979) 415.
[5] D.R. van der Vaart, E.G. Marchand, A. Bagely-Pride, Crit. Rev. Environ. Sci. Technol. 24 (1994) 203.
[6] K. Marr, Environmental Impact Assessment in the United Kingdom and Germany, Ashgate Publ. Ltd., Brookfield, VT, 1997.
[7] R.E. Hester, R.M. Harrison, Volatile Organic Compounds in the Environment, Issues in Environmental Science and Technology, The Royal Society of Chemistry, Cambridge, 1995.
[8] N. Suprenant, T. Nunno, M. Kravett, M. Breton, Halogenated Organic Containing Waste: Treatment Technologies, Noyes Data Corp., Park Ridge, NJ, 1988.
[9] A.A.M. Daifullah, B.S. Girgis, Water Res. 32 (1998) 1169.
[10] T.N. Kalnes, R.B. James, Environ. Prog. 7 (1988) 185.
[11] A.R. Suzdorf, S.V. Morozov, N.N. Anshits, S.I. Tsiganova, A.G. Anshits, Catal. Lett. 29 (1994) 49.
[12] S. Chon, D.T. Allen, AIChE J. 37 (1991) 1730.
[13] J. Frimmel, M. Zdražil, J. Catal. 167 (1997) 286.
[14] E.-J. Shin, A. Spiller, G. Tavoularis, M.A. Keane, Phys. Chem., Chem. Phys. 1 (1999) 3173.
[15] G. Tavoularis, M.A. Keane, J. Chem. Technol. Biotechnol. 74 (1999) 60.
[16] G. Tavoularis, M.A. Keane, J. Mol. Catal. A: Chemical 142 (1999) 187.
[17] J. Estelle, J. Ruz, Y. Cesteros, R. Fernadez, P. Salagre, F. Medina, J.-E. Sueiras, J. Chem. Soc., Faraday Trans. 92 (1996) 2811.
[18] M. Kraus, V. Bazant, in: J. W. Hightower (Ed.), Proceedings of the 5th International Congress on Catalysis, North Holland, Amsterdam, 1969, p. 1073.
[19] B. Coq, G. Ferrat, F. Figueras, J. Catal. 101 (1986) 434.
[20] P. Bodnariuk, B. Coq, G. Ferrat, F. Figueras, J. Catal. 116 (1989) 459.
[21] D.I. Kim, D.T. Allen, Ind. Eng. Chem. Res. 36 (1997) 3019.
[22] E.-J. Shin, M.A. Keane, Appl. Catal. B: Environ. 18 (1998) 241.
[23] E.-J. Shin, M.A. Keane, Chem. Eng. Sci. 54 (1999) 1109.
[24] E.-J. Shin, M.A. Keane, J. Hazard. Mater. B 66 (1999) 265.
[25] B. Hagh, D. Allen, Chem. Eng. Sci. 45 (1990) 2695.
[26] E.J. Creyghton, M.H.W. Burgers, J.C. Jensen, H. van Bekkum, Appl. Catal. A: General 128 (1995) 275.
[27] Y. Ukisu, T. Miyadera, J. Mol. Catal. A: Chem. 125 (1997) 135.
[28] V.I. Simiagina, V.M. Mastikhin, V.A. Yakovlev, I.V. Stoyanova, V.A. Likholobov, J. Mol. Catal. A: Chem. 101 (1995) 237.
[29] J.L. Benitez, G. Del Angel, React. Kinet. Catal. Lett. 66 (1999) 13.
[30] J.B. Hoke, G.A. Gramiccioni, E.N. Balko, Appl. Catal. B: Environ. 1 (1992) 285.
[31] B. Wei, S. Li, H.K. Lee, T.S. Hor, J. Mol. Catal. A: Chem. 126 (1997) L83.
[32] Z. Yu, S. Liao, Y. Xu, React. Funct. Polym. 29 (1996) 151.
[33] M.A. Aramedia, V. Borau, I.M. Garcia, C. Jimenez, J.M. Marinas, F.J. Urbano, Appl. Catal. B: Environ. 20 (1999) 101.
[34] C. Moreau, J. Joffre, C. Saenz, P. Geneste, J. Catal. 122 (1990) 448.
[35] A.R. Suzdorf, S.I. Tsiganova, N.N. Anshits, S.V. Morozov and A.G. Anshits, Sib. Khim. Z. (1992) 131.
[36] A.R. Pinder, Synthesis (1980) 425.

[37] V.V. Lunin, E.S. Lokteva, Russ. Chem. Bull. 45 (1996) 1519.
[38] A. Gampine, D.P. Eyman, J. Catal. 179 (1998) 315.
[39] M.A. Keane, Can. J. Chem. 72 (1994) 272.
[40] B. Coughlan, M.A. Keane, J. Catal. 123 (1990) 364.
[41] M.A. Keane, P.M. Patterson, J. Chem. Soc., Faraday Trans. 92 (1996) 1413.
[42] M.A. Keane, J. Catal. 166 (1997) 347.
[43] D.E. Mears, Ind. Eng. Chem. Proc. Des. Dev. 10 (1971) 543.
[44] M. Howe-Grant (Ed.), Kirk-Othmer Encyclopedia of Chemical Technology, Vol.1, 4th Edition, Wiley, New York, 1991, p. 996.
[45] R.T. Sanderson, Chemical Bonds in Organic Compounds, Sun and Sand Publ., Scottsdale, AZ, 1976.
[46] M. Che, C.O. Bennett, Adv. Catal. 36 (1989) 55.
[47] I.L. Simakova, V.A. Semikolenov, Kinet. Katal. 32 (1991) 989.
[48] S. Kovenklioglu, Z. Cao, D. Shah, R.J. Farrauto, E.N. Balko, AIChE J. 38 (1992) 1003.
[49] J.A. Dean, Handbook of Organic Chemistry, McGraw-Hill, New York, 1987.
[50] Y. Ohtsuka, J. Mol. Catal. 54 (1989) 225.
[51] C. Hoang-Van, Y. Kachaya, S.J. Teichner, Y. Arnaud, J.A. Dalmon, Appl. Catal. 46 (1989) 281.
[52] D.L. Trimm, Catal. Rev.-Sci. Eng. 24 (1977) 67.
[53] R.T.K. Baker, Carbon 27 (1989) 315.
[54] G.C. Bond, Appl. Catal. A: General 149 (1997) 3.
[55] T. Halchev, E. Ruckenstein, J. Catal. 73 (1982) 171.
[56] M. Kisinova, D.W. Goodman, Surf. Sci. 108 (1981) 64.
[57] A. Chambers, R.T.K. Baker, J. Phys. Chem. B 101 (1997) 1621.